USING DIFFERENT TURBULENT VISCOUS MODELS TO INVESTIGATE HYDRODYNAMIC PERFORMANCE OF A DUCTED PROPELLER

Nguyen Chi Cong[1,2], Luong Ngoc Loi[2], Ngo Van He[2*]
[1]Vietnam Maritime University,
[2]Hanoi University of Science and Technology

ABSTRACT
A ducted propeller, also known as a Kort nozzle, is a marine propeller fitted with a non-rotating nozzle. It is used to improve the efficiency of the propeller in some kinds of vessel, for example, fishing vessels, trawlers, push-boats and submarines, with heavily load or propellers with limited diameter. In this article, the authors employed three turbulent viscous models, *RNG k-ε, k-ω SST* and transition *SST k-ω* model, to investigate the flow field surrounding a propeller by using a commercial Computational Fluid Dynamic (*CFD*). The hydrodynamic performance of the ducted propeller system and effects of the different turbulent viscous models on the simulation results are also meticulously analyzed. The propeller, with the diameter of 3,65 m, angular velocity of 200 rpm, boss ratio of 0,1730, is selected to calculate, and the accelerating duct with the cross section of Naca 4415 profile is also studied. By using the CFD, geometry model of the ducted propeller is constructed, meshed, refined and computation. The results of the hydrodynamic performance of the ducted propeller has analyzed by using three turbulent viscous models to be shown. And then, from obtained simulation results, the hydrodynamic performances, pressure distribution, and coefficients of the propeller and duct has been also analyzed and discussed.
Keywords: *ducted propeller; nozzle; turbulent viscous model; CFD; hydrodynamic.*

Received: 19/8/2020; Revised: 14/11/2020; Published: 30/11/2020

SỬ DỤNG MÔ HÌNH RỐI KHÁC NHAU XÁC ĐỊNH ĐẶC TÍNH THỦY ĐỘNG LỰC CHÂN VỊT ỐNG ĐẠO LƯU

Nguyễn Chí Công[1,2], Lương Ngọc Lợi[2], Ngô Văn Hệ[2*]
[1]Trường Đại học Hàng hải Việt Nam,
[2]Trường Đại học Bách khoa Hà Nội

TÓM TẮT
Chân vịt ống đạo lưu được biết đến như một loại ống phun, là một loại thiết bị đẩy sử dụng cho tàu thủy được đặt bên trong một ống bao cố định. Thiết bị này được sử dụng nhằm cải thiện hiệu suất đẩy cho chân vịt đối với một số loại tàu như tàu cá, tàu kéo, tàu ngầm, những loại tàu có trọng tải lớn hay những tàu bị hạn chế về đường kính chân vịt. Trong bài báo này, nhóm tác giả sử dụng ba mô hình rối khác nhau gồm *RNG k-ε, k-ω SST* và *k-ω* transition, để khảo sát dòng bao quanh chân vịt thông qua sử dụng công cụ mô phỏng số thương mại CFD. Các đặc tính thủy động lực của một hệ thống chân vịt ống đạo lưu có kể đến ảnh hưởng của mô hình rối khác nhau trong tính toán mô phỏng sẽ được phân tích cụ thể. Một chân vịt cụ thể có đường kính 3,65m, vận tốc quay 200 vòng/phút, tỷ số truyền 0,1730 được sử dụng trong tính toán, ống đạo lưu với mặt cắt ngang có biên dạng Naca 4415 được sử dụng trong nghiên cứu. Thông qua sử dụng CFD, mô hình chân vịt đạo lưu được xây dựng, chia lưới, hiệu chỉnh lưới và tính toán. Các kết quả về đặc tính thủy động lực của chân vịt đạo lưu được phân tích cụ thể với ba mô hình rối sử dụng khác nhau được trình bày. Tiếp theo, các kết quả thu được gồm các hệ số thủy động lực, phân bố áp suất và các hệ số đặc tính chân vịt và ống đạo lưu sẽ được phân tích và thảo luận.
Từ khóa: *chân vịt ống đạo lưu; ống bao chân vịt; mô hình rối; CFD; thủy động lực*

Ngày nhận bài: 19/8/2020; Ngày hoàn thiện: 14/11/2020; Ngày đăng: 30/11/2020

* Corresponding author. *Email: he.ngovan@hust.edu.vn*
https://doi.org/10.34238/tnu-jst.3510

1. Introduction

Ducted propellers, consisting of an annular duct and a propeller put together, have been used on tugs, push-boats, trawlers, and torpedoes. They have also been used in large vessels like tankers and bulk carriers to improve the hydrodynamic characteristics in heavy conditions. In practically, there are two types of ducts, i.e., accelerating and decelerating ones. In an accelerating duct, the flow velocity is expanded due to hydrodynamic characteristics of the duct and the amount of duct drag force is smaller than the lift force, especially in heavy conditions. The use of an accelerating type of duct combined with the propeller, can lead to lower propeller damage and is a good way to increase propulsive efficiency by axial-losses reduction in a bollard condition. In the contrary, decelerating ducts reduce the propulsive efficiency but they suspend cavitation inception and the hazard of vibration decreases.

The original form of a ducted propeller was invented by Ludwig Kort in 1924 in which the rotor was installed in a long channel passing through the ship hull. The main disadvantage of this configuration was the considerable increase of the frictional resistance due to the presence of the channel. In the course of the time, the outline of the device was improved by transforming the long channel into the nozzle ring characterizing the present day ducted propellers. Finally, Stipa and Kort used the experimental method to prove the increase of the efficiency which can be obtained by ducting the propeller with an accelerating nozzle [1], [2].

Although, for many decades, the design and analysis of ducted propellers was mainly carried out on the basis of extensive experimental method [3]-[7], several theoretical methods have also been employed since the pioneering work of Horn and Amtsberg [8], [9]. Most of these theoretical methods are usually based on the combination of different representations of the velocity field induced by the duct (lumped vortex, thin airfoil theory, panel methods *etc*.) with the one induced by the rotor (actuator disk, lifting line, lifting surface, boundary element methods, *etc*) [10]-[26]. Nowadays, computational fluid dynamic (CFD) based methods have frequently used to study several aspects of the flow around ducted propellers [27]-[32].

In this work, three turbulent *RNG k- ε, k-ω SST*, and transition *SST k-ω* models were employed to predict the hydrodynamic performance of the ducted propeller. The simulation results, such as pressure distribution, velocity field and so on, are discussed, and the effect of the selected turbulent models on the calculation result is also thoroughly examined.

2. Theoretical basis

In analysis of a ducted marine propeller, we use significant non-dimension coefficients that are thrust, torque, and efficiency coefficient. They are functions of advance ratio and can be defined as follows [34], [35]:

$$K_{Tp}=\frac{T_p}{\rho n^2 D^4};K_{Td}=\frac{T_d}{\rho n^2 D^4};K_Q=\frac{Q}{\rho n^2 D^5};J=\frac{V_a}{nD};\eta_0=\frac{\left(K_{Tp}+K_{Td}\right).J}{K_Q.2\pi} \quad (1)$$

Where:

J is the advanced ratio, V_a is the axial velocity, n is the rotating speed, D is the diameter of the propeller, T_p and T_d are the thrusts of propeller and duct, Q is the torque of a propeller, ρ is the density of fluid. K_{tp} and K_{td} are the thrust coefficients of propeller and duct, respectively. K_Q is the torque coefficient of propeller and η_o is the efficiency of the ducted propeller.

To deal with this problem, we usually solve transport equations in moving reference frame to find energy exchange of flow with a machine. In this rotating coordinate system, these equations for the turbulent incompressible flow encountered in this research are the three-dimensional *RANS* equations for the conservation of mass and momentum, given as [33]:

$$\frac{\partial}{\partial x_i}\left(\rho \bar{u}_i\right)=0 \tag{2}$$

$$\frac{\partial}{\partial t}\left(\rho \bar{u}_i\right)+\frac{\partial}{\partial x_j}\left(\rho \bar{u}_i \bar{u}_j\right)=\rho \bar{F}_i-\frac{\partial \bar{p}}{\partial x_j}\left[\mu\left(\frac{\partial \bar{u}_i}{\partial x_j}+\frac{\partial \bar{u}_j}{\partial x_i}\right)\right] \tag{3}$$

Where $\bar{p}$ is the average pressure, μ is the molecular viscosity and $\rho \bar{u}_i \bar{u}_j$ is the Reynolds stress. To correctly account for turbulence, the Reynolds stresses are modeled in order to achieve the closure of Equation (2). An eddy viscosity μ_t is used to model the turbulent Reynolds stresses.

$$-\rho \overline{u_i' u_j'}=\mu_t\left(\frac{\partial \overline{u_i}}{\partial x_j}+\frac{\partial \overline{u_j}}{\partial x_i}\right)-\frac{2}{3}\delta_{ij}.\left(\rho k+\mu_t \frac{\partial \overline{u_i}}{\partial x_i}\right) \tag{4}$$

Where μ_t is the turbulent viscosity and k is the turbulent kinetic energy.

3. Models and boundary conditions

The propeller, four blades operating at the angular velocity of 200 rpm, was investigated. The main variables of the propeller are shown in the Table 1. The accelerating duct, with the cross section of Naca 4415 was used in all calculations.

Table 1. *Main parameters of the propeller*

No	Parameters	Value	Unit
1	Diameter	3,65	m
2	Pitch	2,459	m
3	Revolution	200	rpm
4	Pitch ratio	0,6737	
5	Number of blade	4	
6	Blade thickness ratio	0,0493	
7	Boss ratio	0,1730	
8	Cross section	Naca 66; a = 0,8	

The first stage in simulation process is to build the geometry model for the problem. It plays important role in simulating and affecting directly in calculation results, so you should do your best when creating geometry. In this article, the team used the SolidWorks software, with many advantages in designing complex surfaces and geometry, to create the geometry for all calculations. The next stage is to construct the calculation domain, suitable space surrounding the ducted propeller with appropriate sizes. In this work, the domain is a cylinder, with the length of thirteen times of the propeller's diameter and the diameter of seven times of the propeller's diameter, divided two components: the static domain and rotating domain. In the third step, the domain is imported, meshed, and refined in the Ansys meshing ICEM tool. All domains are meshed by using tetra mesh in which the rotating domain is modeled with smooth mesh, and the static domain takes the coarse, then converted into polyhedral mesh to save calculation time and improve accuracy for simulation results.

The quality of computational mesh plays important role and directly affects the convergence and results of numerical analysis. To determine mesh independence on calculation results, the team employed calculations for six different meshes to specify the suitable number of mesh. These calculations are carried out at the advance ratio J of 0.1 and the dependence of mesh number with the calculation results is shown in the Figure 1. From this figure, the team finally selected the fourth case, with 826876 of polyhedral elements corresponding with 4496103 of mesh nodes for all calculations. The geometry, investigated domain and mesh are presented in the Figures 1 and 2.

The turbulent *RNG k-ε* two equation model is selected as the turbulence viscous model to close Reynolds averaged equations with some detail boundary as follows:

+ Inlet is set as velocity inlet with assumption that it is uniform, axial and its value equals the advance velocity of the ship.

+ Outlet is selected as pressure outlet with the gauge pressure value of 0 *Pa*.

+ Duct is set as wall boundary condition with standard wall function and no slip condition.

+ Propeller is set as moving wall with standard wall function and rough of 5%.

+ Static domain is set as the static zone with fluid

+ The rotating domain is defined as rotational zone with angular velocity of -200 rpm.

+ The first order upwind scheme with numerical under- relaxation is applied for the discretization of the convection term and the central difference scheme is employed for the diffusion term.

+ The pressure - velocity coupling is solved through the PISO algorithm.

+ Convergence precision of all residuals is under 0,0001.

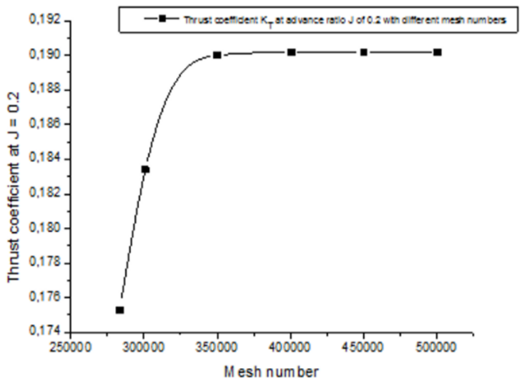

Domain	Nodes	Elements	Polyhedral
Dynamic fluid	1469699	292457	292457
Static fluid	3026404	534419	534419
All Domains	4496103	826876	826876

Figure 1. *Results of mesh independence and detail parameters of mesh*

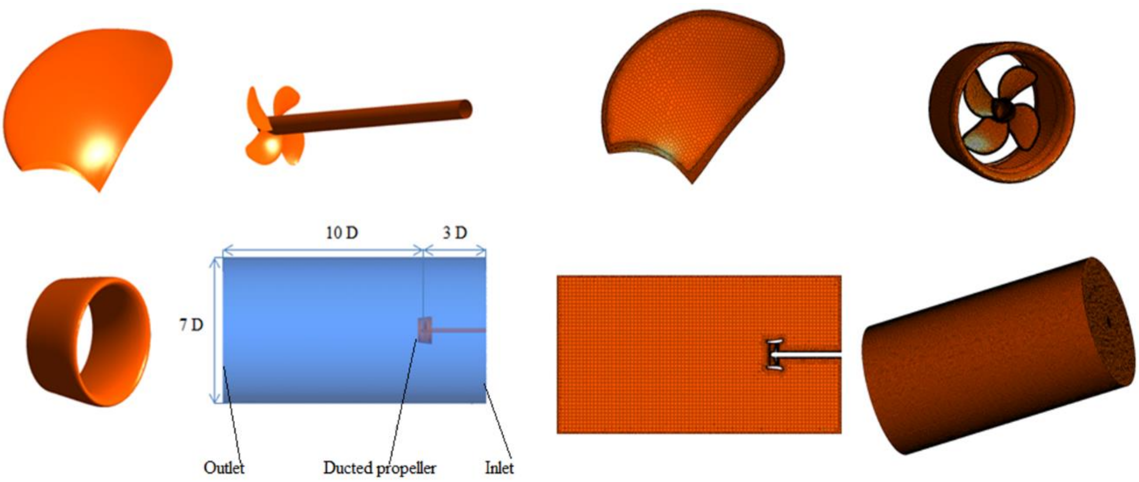

Figure 1. *Duct, propeller, investigated domain and mesh*

4. Results and discussion

Figure 3 shows the pressure distribution on the propeller blade's faces at advance ratio J of 0,1; 0,4 and changing principle of thrust coefficients. As we can be seen from this figure that the pressure value of the pressure face is higher than that of the back face. In the results of computation at the advance ratio J of 0,1 and 0,4 the maximum value on the pressure face is about 24000 Pa, and almost area of it takes the pressure value of 8000 Pa, while the maximum, in the back face, is about 8000 Pa, and almost area of it is about the value of - 4500 Pa. Moreover, at the blade's tip of the back face, the value is relatively low about -120000 Pa. This pressure difference between two faces makes the propeller's thrust. The changing law of the propeller's coefficients with the advance ratio *J* is also presented in the figure. In addition, we recognize from this figure that thrust coefficient considerably decreases when the advance ratio *J* goes up. The maximum of thrust coefficients is at advance ration J of 0,1 in the range of the advance ratio J from 0,1 to 0,55 as shown.

Fig. 4 describes the pressure distribution on the duct and its thrust coefficient at various advance ratios. In general, the cross section of a duct has the shape of an airfoil, so when a duct interacts with the flow generates difference in pressure distribution on two faces of a duct, low pressure inside the duct and high pressure outside the duct. As consequence of this, hydrodynamic force is made on the duct and divided into two components; one has the same direction of propeller's thrust, the other is particular with the propeller's axis. Thus, the total thrust of the ducted propeller system is sum of the thrust made by the duct and the thrust of the propeller. Moreover, from this figure, we can see that when the advance ratio raises, the thrust coefficient of the duct significantly declines, and it's maximum value is 0,13 at the advance ratio *J* of 0,1. At the *J* of 0,55, its thrust coefficient reaches the minimum value about -0,01, so the duct's thrust causes the thrust reduction of the system. From above analyses, we can make a conclusion that the ducted propeller is appropriate with the vessel operating in small velocity and heavy load.

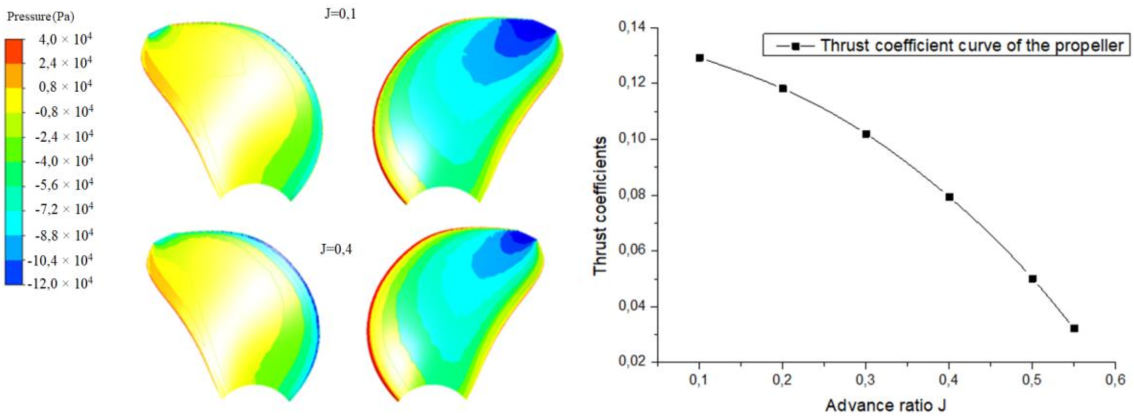

Figure 3. *Pressure distribution faces of propeller at J of 0,1; 0,4 and changing law of propeller's thrust coefficient*

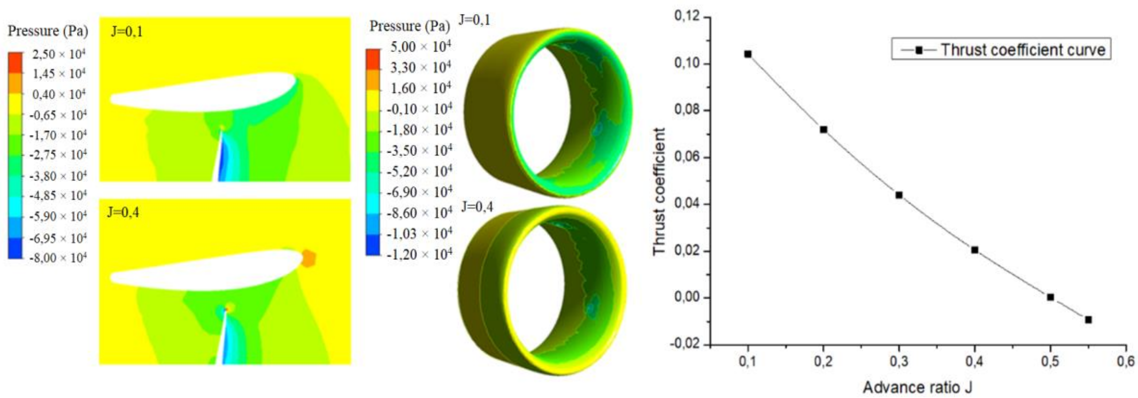

Figure 2. *Pressure distribution on the duct at J =0,1; 0,4 and changing law of thrust coefficients*

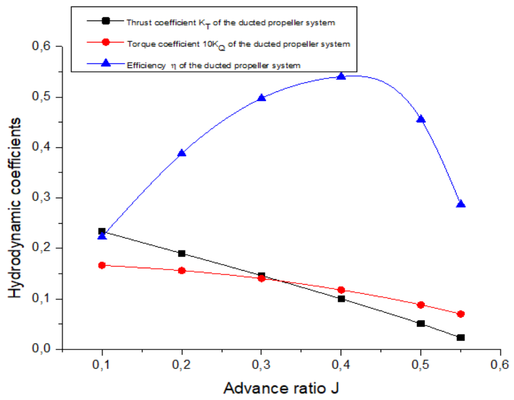

Figure 5. *Thrust, torque, efficiency coefficient of the ducted propeller*

The hydrodynamic performance of the ducted propeller is shown in Figure 5. As can be seen in the figure that changing law of thrust and torque coefficients of the ducted propeller system is the same as a linear function of the advance ratio *J*. These factors reaching the maximum value is 0,23 and 0,17 at the advance ratio *J* of 0.1 respectively. On the other hand, the efficiency of the system changes in a curve of the advance ratio *J*, and gets the maximum value of 0,54 at the *J* of 0,4.

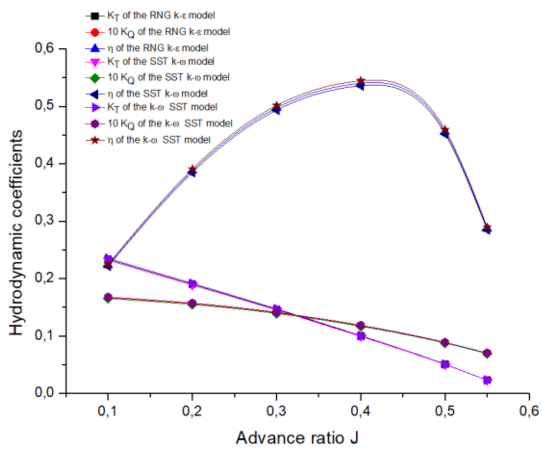

Figure 7. *Hydrodynamic performance of the ducted propeller with different turbulent models*

The obtained results with three different turbulent models presented in the Figure 7 reveals that the selected turbulence models have the slight impact on the calculation results. With the *k - ω SST* model, the propeller's efficiency gets the maximum value about 0,545 while the minimum efficiency of the studied propeller is about 0.536 with the transition *SST k - ω* model corresponding with the advance ratio *J* of 0,4. In the same way, thrust coefficient of the propeller gets the maximum about 0,1133 with the transition *SST k - ω* model and the minimum about 0,1129 in the *RNG k - ε* model. With the propeller's torque coefficient, the maximum and minimum values are about 0,133; 0,1317 respectively corresponding with the model and the transition *SST* model. However, the error of the investigated parameters among the selected models, being relatively small about 1,39 %, can be negligible in the calculation.

5. Conclusion

In this study, numerical investigation and analysis of steady flows around and the ducted propeller at the different ratios have been presented. An unstructured grid based on *RANS* was applied to investigate the ducted propeller's hydrodynamic performance. Here are some important conclusions of this paper.

+ The four-bladed skewed propeller of the ducted propeller system is selected for verification of numerical simulation and ducted propeller. The numerical predictions of thrust, torque and efficient coefficient with different advance ratios are carried out. Obtained results show that the efficiency of propeller increases dramatically at the small ratios and the numerical prediction results are in good agreement with the theoretical prediction.

+ Pressure distribution on the duct and blade was presented in contours. Negative low pressure was presented in back side and high positive pressure was given in face side of the blade. Lower pressure at suction side of the duct (inside of the duct) was also observed.

+ Three turbulence models were employed to investigate the effects of different turbulence models on the simulation results. The achieved outcomes suggest that the chosen turbulence models have the inconsiderable effect on the simulation results, and can ignore.

REFERENCES

[1]. L. Stipa, “Ala a turbina,” *L’Aerotecnica*, vol. 12, no. 10, pp. 653-674, 1931.

[2]. L. Kort, “Der neue dusenschrauben-antrieb,” *Werft, Reederei und Hafen*, vol. 15, pp. 1-15, 1934.

[3]. J. D. Van Manen, “Recent research on propellers in nozzles,” *International Shipbuilding Progress*, vol. 4, no. 36, pp. 395-424, 1957.

[4]. J. D. Van Manen, and A. Superina, “The design of screw propellers in nozzles,” *International Shipbuilding Progress*, vol. 6, no. 55, pp. 95-113, 1959.

[5]. J. D. Van Manen, “Effect of radial load distribution on the performance of shrouded propellers,” *Transaction RINA*, vol. 9 no. 93, pp. 185-196, 1962.

[6]. J. D. Van Manen, and M. W. C. Oosterveld, “Analysis of ducted propeller design,” *Transaction SNAME*, vol. 74, pp. 522-561, 1966.

[7]. M. W. C. Oosterveld, *Wake adapted ducted propellers*, Technical Report no. 345 at Netherlands Ship Model Basin, pp. 1-130, 1970.

[8]. F. Horn, “Beitrag zur theorie ummantelter schiffsschrauben,” *Jahrbuch der schiffbautechnischen Gesellschaft*, vol. 2, pp. 106-187, 1940.

[9]. F. Horn, and H. Amtsberg, “Entwurf von schiffsdusen systemen (kortdusen),” *Jahrbuch der schiffbautechnischen Gesellschaft*, vol. 44, pp. 141-206, 1950.

[10]. D. Ktichemann, and J. Weber, *Aerodynamics of propulsion*. McGraw-Hill, 1953.

[11]. A. J. Tachmindji, “The potential problem of the optimum propeller with finite number of blades operating in a cylindrical duct,” *Journal of Ship Research*, vol. 2, no. 3, pp. 23-32, 1958.

[12]. D. E. Ordway, M. M. Sluyter, and B. O. U. Sonnerup, *Three-dimensional theory of ducted propellers*, UNCLASSIFIED AD, 1960.

[13]. W. B. Morgan, *A theory of the ducted propeller with a finite number of blades*, Technical Report of University of California, 1961.

[14]. W. B. Morgan, “Theory of the annular airfoil and ducted propeller,” *Proceedings of the Fourth Symposium on Naval Hydrodynamics*, 1962, pp. 151-197.

[15]. G. A. Dyne, *A method for the design of ducted propellers in a uniform flow*, Technical Report no. 62; Swedish state Shipbuiding Experimental Tank, 1967.

[16]. P. G. Ryan, and E. J. Glover, “A ducted propeller design method: a new approach using surface vorticity distribution techniques and lifting line theory,” *Trans RINA*, vol. 114, pp. 545-563, 1972.

[17]. W. B. Morgan, and E. B. Caster, “Comparison of theory and experiment on ducted propellers,” *Proceedings of the 7th Symposium on Naval Hydrodynamics*, 1968, pp. 1311-1349.

[18]. N. Caracostas, “Off design performance analysis of ducted propellers,” *Proceedings Propellers/Shafting ’78 Symposium, SNAME*, 1978, pp. 31-38.

[19]. S. Tsakonas, W. R. Jacobs, and M. R. Ali, “Propeller-duct interaction due to loading and thickness effects,” *Proceedings of the Propellers/Shafting ’78 Symposium, SNAME*, 1978.

[20]. R. Van Houten, *Analysis of ducted propellers in steady flow*, Technical Report, Airflow Research and Manufacturing Corp, 1986.

[21]. J. E. Kerwin, S. A. Kinnas, J. T. Lee, and W. Shih, “A surface panel method for the hydrodynamic analysis of ducted propellers,” *Trans SNAME*, vol. 95, pp.1-22, 1987.

[22]. S. A. Kinnas, and W. B. Coney, “On the optimum ducted propeller loading,” *Proceedings Propellers ’88 Symposium*, 1988, pp. 1.1-1.13.

[23]. W. B. Coney, “A method for the design of a class of optimum marine propulsors,” Ph.D. thesis, Massachusetts Institute of Technology, 1989.

[24]. S. A. Kinnas, and W. B. Coney, “The generalised image model - an application to the design of ducted propellers,” *Journal of Ship Research*, vol. 36, pp. 197-209, 1992.

[25]. J. Baltazar, and J. A. C. Falcao de Campos, “On the modelling of the flow in ducted propellers with a panel method,” *Proceedings of the 1st International Symposium on Marine Propulsors*, 2009, vol. 9, pp. 1-15.

[26]. F. Celik, M. Guner, and S. Ekinci, “An approach to the design of ducted propeller,” *Transaction B: Mechanical Engineering, Scientia Iranica*, vol. 17, no. 5, pp. 406-417, 2010.

[27]. M. Abdel-Maksoud, and H. J Heinke, “Scale effects on ducted propellers,” *Proceedings of the 24th Symposium on Naval Hydrodynamics*, 2002, pp. 1-16.

[28]. J. Kim, E. Paterson and F. Stern, "Sub-visual and acoustic modeling for ducted marine propulsor," *Proceedings of the 8th International Conference on Numerical Ship Hydrodynamics*, 2003, pp. 22-25.

[29]. T. Wang, L. D. Zhou, and X. Zhang, "Numerical simulation of 3-D integrative viscous complicated flow field around axisymmetric body with ducted propulsion," *Journal of Ship Mechanics*, vol. 7, no. 2, pp. 21-32, 2003.

[30]. M. Hoekstra, "A rans-based analysis tool for ducted propeller systems in open water condition," *International shipbuilding progress*, vol. 53, no. 3, pp. 205-227, 2006.

[31]. A. Sanchez-Caja, J. V. Pylkkanen, and T. P. Sipila, "Simulation of the incompressible viscous flow around ducted propellers with rudders using a ranse solver," *Proceeding of the 27th Symposium on Naval Hydrodynamics*, 2008, pp. 1-11.

[32]. H. Haimov, J. Vicario, and J. Del Corral, "Ranse code application for ducted and endplate propellers in open water," *Proceedings of the Second International Symposium on Marine Propulsors*, 2011, pp. 1-9.

[33]. ANSYS, Inc, *ANSYS Fluent Theory Guide*, 2013, vol. 14.0, pp. 1-814.

[34]. J. Carlton, *Marine Propellers and Propulsion*, Butterworth, Heinemann, 2012, pp. 1-544.

[35]. P. John, and P. A. Breslin, *Hydrodynamics Of Ship Propellers*. Cambridge University Press, 1993, pp. 1-600.